PNAS
www.pnas.org

Supplementary Information for

Current water quality guidelines across North America and Europe do not protect lakes from salinization

William D. Hintz*, Shelley E. Arnott, Celia C. Symons, Danielle A. Greco, Alexandra McClymont, Jennifer A. Brentrup, Miguel Cañedo-Argüelles, Alison M. Derry, Amy L. Downing, Derek K. Gray, Stephanie J. Melles, Rick A. Relyea, James A. Rusak, Catherine L. Searle, Louis Astorg, Henry K. Baker, Beatrix E. Beisner, Kathryn L. Cottingham, Zeynep Ersoy, Carmen Espinosa, Jaclyn Franceschini, Angelina T. Giorgio, Norman Göbeler, Emily Hassal, Marie-Pier Hébert, Mercedes Huynh, Samuel Hylander, Kacie L. Jonasen, Andrea E. Kirkwood, Silke Langenheder, Ola Langvall, Hjalmar Laudon, Lovisa Lind, Maria Lundgren, Lorenzo Proia, Matthew S. Schuler, Jonathan B. Shurin, Christopher F. Steiner, Maren Striebel, Simon Thibodeau, Pablo Urrutia-Cordero, Lidia Vendrell-Puigmitja, Gesa A. Weyhenmeyer

*Corresponding author: William D. Hintz.
Email: William.Hintz@utoledo.edu or hintzwd@gmail.com

Data Availability: Data, supporting files, and metadata can also be found in the Scholars Portal Dataverse archive at: https://doi.org/10.5683/SP3/BIDMCI (Arnott et al. 2021)

This PDF file includes:

APPENDIX 1

Supplemental Methods Text

For each experiment, we filled the mesocosms, which ranged in size from 80 to 2500 L, with water that was filtered through a 40- to 100-µm mesh to remove most zooplankton but allow small, edible phytoplankton to pass through. The water source was a local lake for 13 of the experiments; in the remaining cases, we used water from a lake outflow (Convict) or well water (Purdue, Dartmouth). We measured total phosphorus (TP), total nitrogen (TN), calcium (Ca^{2+}), Cl^-, and conductivity by either a) taking a water sample from the lake, b) using a composite sample from multiple mesocosms at the beginning of the experiment, or c) by using existing data from prior analyses from long-term monitoring programs (see SI Appendix 1, Table 1.1 for water conditions for each study site). After allowing the phytoplankton communities to acclimate for a few days, we collected zooplankton from the same lake where water was collected or a nearby pond when well water was used, using the same mesh size used to filter the mesocosm water. An aliquot of zooplankton was added to each mesocosm to recreate the same community composition and abundance as in the source lake or pond. To prevent declines in zooplankton abundance due to food limitation in the mesocosms, we added nitrogen (NH_4NO_3) and phosphorus (KH_2PO_4) to 13 of the experimental sites at weeks 2 and 4 to replace nutrients, assuming an estimated loss of 5% per day from the water column due to periphyton growth and sedimentation (1).

One to nine days after we stocked the zooplankton, we added NaCl to achieve the nominal experimental concentrations (SI Appendix 2, Table 2.1). Initial day (day 1) and final (day 41 – 51) Cl^- concentrations were determined either by measuring Cl^- directly or estimating Cl^- indirectly using conductivity (SI Appendix 3, Tables 3.1). Nominal and actual Cl^- concentrations differed by 5-28% (SI Appendix 3, Tables 3.2). Chloride concentrations sometimes varied over time due to rainfall and evaporation in the mesocosms, therefore we used the average Cl^- values between initial and final samples for all statistical analyses (SI Appendix 3, Figs. 3.1 – 3.2). We also measured several abiotic variables during the experiment including water temperature, conductivity, pH, and dissolved oxygen.

References

1. A. L. Downing *et al.*, Environmental fluctuations induce scale-dependent compensation and increase stability in plankton ecosystems. *Ecology* 89:3204-3214 (2008).

Table 1.1. Location and characteristics of source lakes and experimental approach. Latitude (Lat) and Longitude (Long) are given in decimal degrees, mesocosm volume (Vol), n is the number of mesocosms used in the experiment, Start and End are the dates in 2018 when the experiments were conducted, chloride (Cl), calcium (Ca), total nitrogen (TN), total phosphorus (TP), and chlorophyll a (Chl *a*) concentration represent source water values.

Lake	Country	Lat	Long	Venue	Vol (L)	n	Start (DD-MM)	End (DD-MM)	Duration (days)	Cl (mg/L)	Ca (mg/L)	TN (ug/L)	TP (ug/L)	Chl *a* (ug/L)	pH
Paint	Canada	45.22	-78.94	land	800	30	28-06	08-09	42	17.5	4.7	210	8.4	0.58	7.0
Long	Canada	44.53	-76.39	lake	1570	30	22-06	02-08	49	0.41	34.7	330	13.6	0.34	8.1
Dartmouth	USA	43.73	-72.25	land	120	21	25-07	06-09	43	9.7	19.7	187	7	1.81	7.6
Sturgeon	Canada	44.46	-78.67	land	200	30	30-06	11-08	43	14.8	26.2	540	9.2	3.76	8.1
Purdue	USA	40.45	-87.05	land	150	30	13-09	31-10	42	1.62	59.2	570	66.8	2.68	7.8
Stortjärn	Sweden	64.15	19.45	lake	550	20	26-06	07-08	42	0.63	3.8	305	11	2.2	5.2
Croche	Canada	45.99	-74.00	lake	2500	20	22-06	03-08	42	0.26	2.74	210	6.7	0.31	6.2
George	USA	43.34	-73.38	land	1000	30	10-07	21-08	41	18	11	125	4	1.8	7.6
Opeongo	Canada	45.70	-78.36	land	180	30	29-06	11-08	42	1.74	2.58	340	11.8	6	7.1
Kraus	USA	40.20	-83.06	land	300	32	06-07	24-07	42	1	5.51	2740	120	14.7	8.6
Hertel	Canada	45.54	-73.22	land	80	20	26-06	08-08	43	0.895	10.72	275	23	5.6	7.4
KBS	USA	42.40	-85.41	land	345	21	28-06	09-08	42	8.86	33.2	1320	10.3	1.65	9
Feresjön	Sweden	57.17	14.81	lake	550	20	03-07	14-08	42	6.52	4.68	320	1.49	2.02	7.6
Erken	Sweden	59.84	18.58	lake	550	20	26-06	10-08	46	11	42.9	624	23.8	1.07	7.9
Convict	USA	37.58	-118.85	land	1000	30	13-07	23-08	51	0.45	26.3	110	7	0.23	8.6

Tavernoles	Spain	41.95	2.31	land	200	20	11-08	20-12	42	11.3	75	8110	530	9.93	7.7
MEDIAN					447.5	25.5			42	4.1	15.4	325	10.6	1.9	7.6
MEAN					631	25			43.4	6.5	22.7	1019	53.4	3.4	8.0
STDEV					645.9	5			2.8	6.6	21.8	2000	130.7	3.9	0.9

APPENDIX 2

Table 2.1. Nominal chloride concentrations and the mass of NaCl added (on a per liter basis) for 20- and 30-mesocosm experiments.

30 mesocosms			*20 mesocosms*		
Enclosure	**Cl^- mg/L**	**NaCl mg/L**	**Enclosure**	**Cl^- mg/L**	**NaCl mg/L**
1	0	0	1	0	0
2	10	16.48	2	20	32.97
3	20	32.97	3	40	65.94
4	40	65.94	4	60	98.91
5	60	98.91	5	80	131.88
6	80	131.88	6	100	164.85
7	100	164.85	7	150	247.27
8	120	197.81	8	200	329.69
9	140	230.78	9	250	412.11
10	160	263.75	10	300	494.54
11	200	329.69	11	400	659.38
12	250	412.11	12	500	824.23
13	300	494.54	13	600	989.07
14	350	576.96	14	700	1153.92
15	400	659.38	15	800	1318.76
16	450	741.80	16	900	1483.61
17	500	824.23	17	1000	1648.45
18	550	906.65	18	1100	1813.30
19	600	989.07	19	1300	2142.99
20	650	1071.49	20	1500	2472.68
21	700	1153.92			
22	750	1236.34			
23	800	1318.76			
24	850	1401.18			
25	900	1483.61			
26	1000	1648.45			
27	1100	1813.30			
28	1200	1978.14			
29	1300	2142.99			
30	1500	2472.68			

APPENDIX 3

Conversion of conductivity to chloride

For three of the sixteen experiments (KBS, Kraus, Sturgeon) we lacked direct Cl^- measurements. For these experiments we used conductivity measurements to estimate initial (week 0) and final (week 6) Cl^- concentrations. We calculated regressions between conductivity and nominal Cl^- levels and then used the regressions to convert initial and final conductivity measures into predicted Cl^- (Figure 3.1). To determine the accuracy of this method, we used the same regression method for experiments that had both initial conductivity and Cl^- measurements. We used initial measurements because we assumed actual and nominal Cl^- values would be the closest shortly after NaCl addition, before rainfall and evaporation effects. We then regressed predicted Cl^- values versus actual Cl^- as measured in the mesocosms. In Table 3.1, we report the R-squared values and the average absolute difference in mg Cl^-/L for 'actual estimated Cl^-' vs 'actual Cl^-' for all experiments that had initial conductivity and Cl^- measurements. In control tanks (no Cl^- added) for Kraus and KBS, the regression method estimated small negative Cl^- values. We replaced these negative values for the controls with 0 mg Cl^-/l.

Observations from experiments that had actual Cl^- estimates for week 0 and 6 showed changes in Cl^-, in some cases due to known instances of high evaporation or rainfall (Figure 3.2). To account for variable Cl^- values over the six-week period, we predicted Cl^- values from conductivity using the regression method for experiments that did not have both initial and final Cl^- values. For Feresjön, initial Cl^- values were only available for week 3, not week 0. For Croche, only initial actual Cl^- values were used for week 0 because predicted Cl^- values for final Cl^- were overestimated at low concentrations, and observations of Cl^- and conductivity for both in-lake mesocosms showed very little change over time. We expect evaporation and rainfall effects on chloride to be much smaller for in-lake mesocosms due to larger volumes and lower temperature fluctuations compared to land-based mesocosms.

Nominal versus actual Cl^- *comparisons*

To estimate the accuracy of our Cl^- levels compared to our target (i.e., nominal) values, we calculated the percent deviation of Cl^- levels for each mescososm in week 0 (Figure 3.3). This value was calculated as: $\frac{|actual\ chloride - nominal\ chloride|}{nominal\ chloride}$
We then calculated the average and standard deviation of the percent deviation for each lake (Table 3.2).

Table 3.1. Results of the analysis to describe error in predicting Cl^- concentrations using conductivity levels in mesocosms. The R-squared values represent the fit between predicted Cl^- concentrations and actual Cl^- concentrations for lakes that had both conductivity and Cl^- data. The mean difference shows the error in predicting Cl^- concentrations for each mesocosm when using conductivity. The mesocosm volume and venue are also included to provide context for potential sources of error when constructing the conductivity-nominal Cl^- relationship used to predict actual Cl^- concentrations.

Lake	R-squared	Mean difference (mg/L Cl^-)	Mesocosm volume (L)	Venue
Paint	0.998	-23.473	800	Land-based
Long	0.996	54.264	1570	In-lake
Purdue	0.973	-3.420	150	Land-based
Stortjärn	0.974	109.663	550	In lake
Croche	0.986	102.377	2500	In-lake
George	0.993	-33.051	1000	Land-based
Opeongo	0.994	45.041	180	Land-based
Hertel	0.996	27.848	80	Land-based
Erken	0.995	1.983	550	In lake
Tavernoles	0.886	-186.450	200	Land-based

Table 3.2. Values of average and standard deviation (SD) of the percent deviation from the nominal Cl^- levels in week 0 across lakes.

Lake	Average percent deviation	SD of the percent deviation
Paint	26.43	38.36
Long	13.29	6.35
Dartmouth	10.14	14.4
Sturgeon	7.7	7.92
Purdue	4.75	10.14
Stortjärn	23.31	18.43
Croche	23.23	14.82
George	17.34	33.8
Opeongo	9.12	5.26
Kraus	25.22	53.51
Hertel	6.77	3.64
KBS Reservoir	10.85	25.47
Feresjön*	8.76	9.09
Erken	9.95	14.58
Convict	28.19	19.17
Tavernoles	13.64	25.78

*based on initial Cl^- in week 3

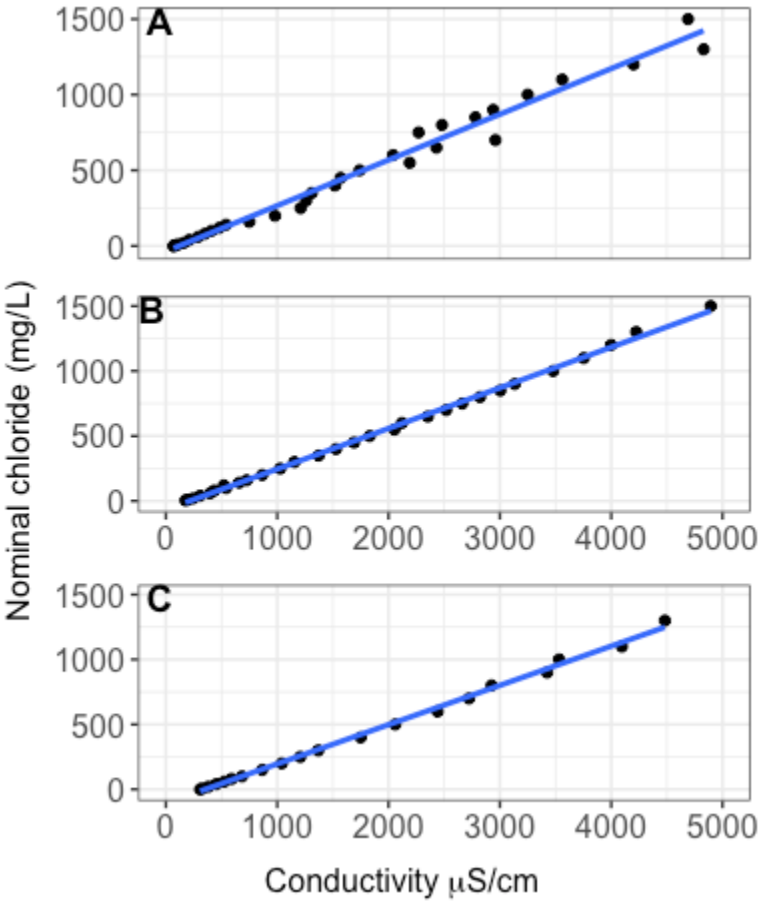

Figure 3.1. Relationship between conductivity and nominal Cl^- concentrations for (A) Kraus Lake, (B) Sturgeon Lake, and (C) KBS Reservoir using data collected at week 0 (initial) in the experiments. The R-squared values for all fits were >0.98.

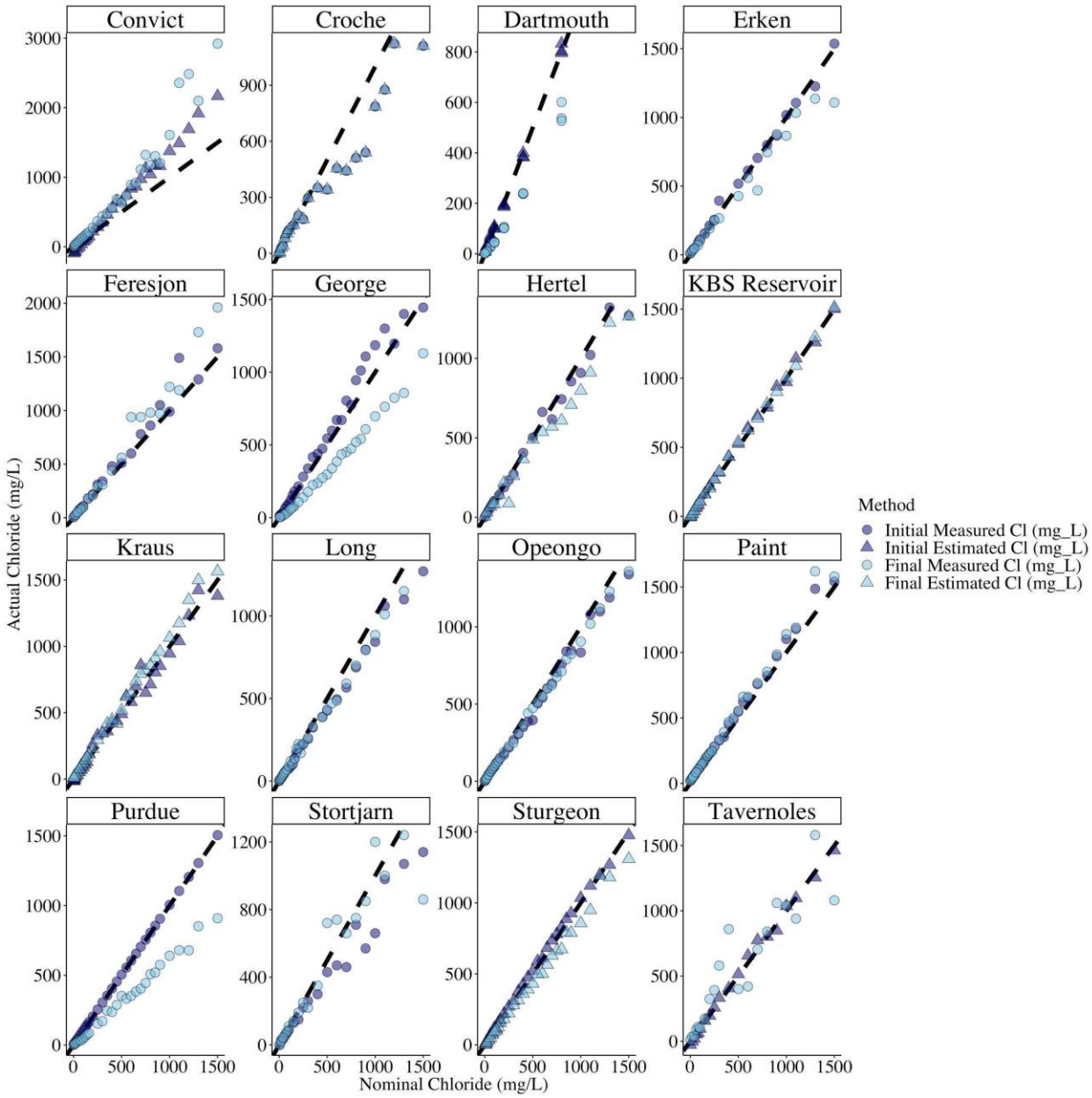

Figure 3.2. Relationship between nominal Cl^- concentrations actual Cl^- values. Initial chloride measurements from week 0 = gray, final chloride measurements from week 6 = light blue. Circles represent actual Cl^- measurements. Triangles represent estimated Cl^- values from conductivity values. The 1:1 ratio is indicated with a dashed line. Feresjön initial Cl^- measurements are from week 3. Croche final measurements are not shown because they were not used in the averaged Cl^- measurements due to errors in estimation at low nominal Cl^- levels.

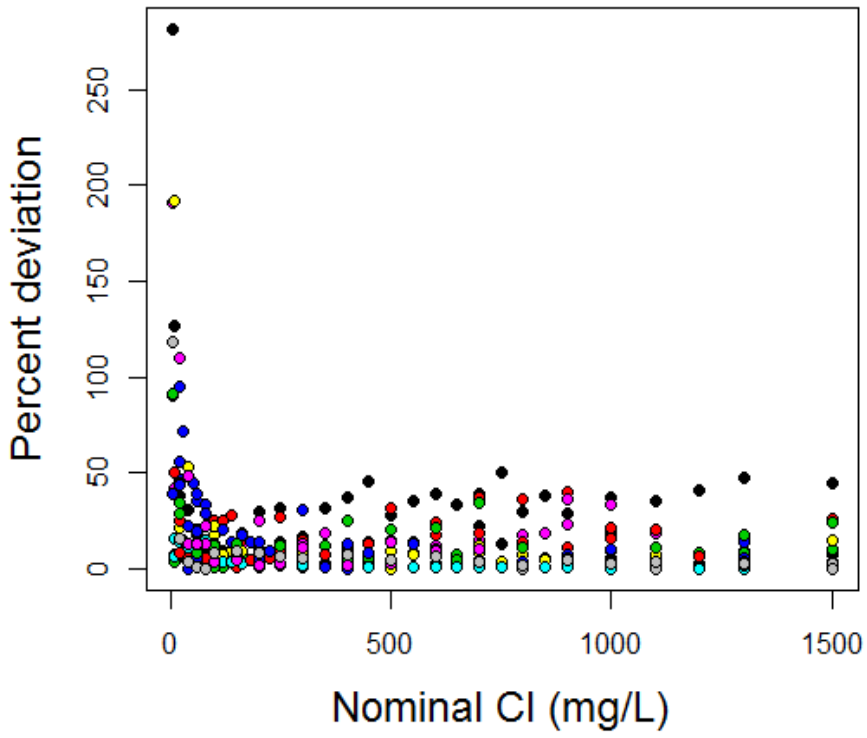

Figure 3.3. Percent deviation of actual Cl^- values from nominal concentrations. Data are shown for each lake (coded by color) in week 0.

APPENDIX 4

Individual site responses of calanoid copepods, cyclopoid copepods, rotifers, and chlorophyll *a* to Cl^- gradients (cladoceran figure reported in main paper).

Table 4.1. Model comparison table for cladoceran abundance in the 16 study sites, including delta AICc and adjusted R^2 values and whether the relationship was used to predict an LC_{50}. For consistency, we only used GAM models with log(abundance + 1) to predict LC_{50} (in bold). The "Used for LC_{50}" column indicates if there was enough data and the shape of the curve permitted us to calculate LC_{50} (see methods for more details). Models considered included linear (lm) and generalized additive (gam) models with abundance (ab), log(abundance + 1) (logab), log(Cl^- concentration + 1) (logcl), and both variables log-transformed (loglog). Table shows models within 2 ΔAIC and GAM models with log(abundance + 1).

Lake	Model	Delta AICc	Adjusted R^2	Used for LC_{50}
Paint	**gam.logab**	**0.00**	**0.777**	**Y**
Long	lm.loglog	0.00	0.441	N
Long	**gam.logab**	**2.15**	**0.459**	**Y**
Dartmouth	lm.logab	0.00	0.720	N
Dartmouth	**gam.logab**	**0.80**	**0.726**	**Y**
Sturgeon	lm.logab	0.00	0.640	N
Sturgeon	**gam.logab**	**0.87**	**0.672**	**Y**
Purdue	lm.logab	0.00	0.762	N
Purdue	**gam.logab**	**0.77**	**0.766**	**Y**
Stortjärn	**gam.logab**	**0.00**	**0.879**	**Y**
Croche	**gam.logab**	**0.00**	**0.837**	**Y**
George	lm.logab	0.00	0.582	N
George	**gam.logab**	**0.90**	**0.607**	**Y**
Opeongo	lm.logab	0.00	0.218	N
Opeongo	**gam.logab**	**0.00**	**0.218**	**Y**
Kraus	lm.logab	0.00	0.774	N

Kraus	**gam.logab**	**0.00**	**0.774**	**Y**
Hertel	lm.logab	0.00	0.556	N
Hertel	**gam.logab**	**0.82**	**0.565**	**Y**
KBS Reservoir	**gam.logab**	**0.00**	**0.929**	**Y**
Feresjön	lm.logab	0.00	0.687	N
Feresjön	**gam.logab**	**2.07**	**0.796**	**Y**
Erken	lm.logab	0.00	0.251	N
Erken	**gam.logab**	**0.20**	**0.429**	**Y**
Convict	**gam.logab**	**0.00**	**0.782**	**Y**

Table 4.2. Model comparison table for cyclopoid copepod abundance in the 16 study sites, including delta AICc and adjusted R^2 values and whether the relationship was used to predict an LC_{50}. For consistency, we only used GAM models with log(abundance + 1) to predict LC_{50} (in bold). The "Used for LC_{50}" column indicates if there was enough data and the shape of the curve permitted us to calculate LC_{50} (see methods for more details). Models considered included linear (lm) and generalized additive (gam) models with abundance (ab), log(abundance + 1) (logab), log(Cl^- concentration + 1) (logcl), and both variables log-transformed (loglog). Table shows models within 2 ΔAIC and GAM models with log(abundance + 1).

Lake	Model	Delta AICc	Adjusted R^2	Used for LC_{50}
Paint	**gam.logab**	**0.00**	**0.934**	**Y**
Long	lm.loglog	0.00	0.369	N
Long	**gam.logab**	**6.75**	**0.297**	**N**
Dartmouth	lm.logab	0.00	0.047	N
Dartmouth	**gam.logab**	**0.14**	**0.049**	**Y**
Dartmouth	lm.loglog	1.29	-0.013	N
Sturgeon	**gam.logab**	**0.00**	**0.895**	**Y**
Purdue	lm.logab	0.00	-0.033	N
Purdue	lm.loglog	0.07	-0.036	N
Purdue	**gam.logab**	**0.68**	**0.020**	**N**
Stortjärn	lm.loglog	0.00	0.492	N
Stortjärn	**gam.logab**	**2.22**	**0.653**	**Y**
Croche	lm.loglog	0.00	0.315	N
Croche	**gam.logab**	**6.95**	**0.184**	**Y**
George	lm.loglog	0.00	0.119	N
George	lm.logab	0.33	0.110	N
George	**gam.logab**	**0.33**	**0.110**	**Y**
Opeongo	**gam.logab**	**0.00**	**0.585**	**Y**

Opeongo	lm.logab	0.05	0.526	N
Kraus	lm.logab	0.00	0.496	N
Kraus	**gam.logab**	**0.00**	**0.496**	**Y**
Hertel	lm.logab	0.00	0.039	N
Hertel	**gam.logab**	**0.00**	**0.039**	**N**
Hertel	lm.loglog	0.69	0.005	N
KBS Reservoir	**gam.logab**	**0.00**	**0.806**	**Y**
Feresjön	**gam.logab**	**0.00**	**0.907**	**Y**
Erken	lm.loglog	0.00	0.036	N
Erken	lm.logab	0.50	0.009	N
Erken	**gam.logab**	**0.50**	**0.009**	**Y**
Convict	**gam.logab**	**0.00**	**0.427**	**Y**
Convict	lm.logab	0.47	0.335	N
Tavernoles	lm.logab	0.00	0.407	N
Tavernoles	**gam.logab**	**0.00**	**0.407**	**Y**

Table 4.3. Model comparison table for calanoid copepod abundance in the 16 study sites, including delta AICc and adjusted R^2 values and whether the relationship was used to predict an LC_{50}. For consistency, we only used GAM models with log(abundance + 1) to predict LC_{50} (in bold). The "Used for LC_{50}" column indicates if there was enough data and the shape of the curve permitted us to calculate LC_{50} (see methods for more details). Models considered included linear (lm) and generalized additive (gam) models with abundance (ab), log(abundance + 1) (logab), log(Cl^- concentration + 1) (logcl), and both variables log-transformed (loglog). Table shows models within 2 ΔAIC and GAM models with log(abundance + 1).

Lake	Model	Delta AICc	Adjusted R^2	Used for LC_{50}
Paint	lm.loglog	0.00	0.188	N
Paint	lm.logab	1.21	0.152	N
Paint	**gam.logab**	**1.82**	**0.206**	**N**
Dartmouth	lm.logab	0.00	0.352	N
Dartmouth	**gam.logab**	**0.72**	**0.402**	**Y**
Sturgeon	lm.loglog	0.00	0.196	N
Sturgeon	**gam.logab**	**1.88**	**0.236**	**N**
Stortjärn	lm.logab	0.00	0.085	N
Stortjärn	**gam.logab**	**0.00**	**0.085**	**N**
Stortjärn	lm.loglog	1.03	0.037	N
Croche	lm.loglog	0.00	0.859	N
Croche	**gam.logab**	**17.28**	**0.813**	**Y**
George	lm.logab	0.00	0.056	N
George	**gam.logab**	**0.00**	**0.056**	**N**
George	lm.loglog	1.26	0.015	N
Opeongo	lm.logab	0.00	0.221	N
Opeongo	**gam.logab**	**0.95**	**0.246**	**Y**
Opeongo	lm.loglog	1.80	0.165	N
Kraus	lm.loglog	0.00	0.574	N

Kraus	**gam.logab**	**0.31**	**0.711**	**N**
KBS Reservoir	lm.loglog	0.00	0.787	N
KBS Reservoir	**gam.logab**	**18.06**	**0.603**	**Y**
Feresjön	lm.loglog	0.00	0.625	N
Feresjön	**gam.logab**	**2.75**	**0.727**	**Y**
Erken	lm.loglog	0.00	0.674	N
Erken	**gam.logab**	**10.95**	**0.576**	**Y**
Convict	lm.loglog	0.00	0.463	N
Convict	**gam.logab**	**15.80**	**0.183**	**N**

Table 4.4. Model comparison table for rotifer abundance in the 16 study sites, including delta AICc and adjusted R^2 values and whether the relationship was used to predict an LC_{50}. For consistency, we only used GAM models with log(abundance + 1) to predict LC_{50} (in bold). The "Used for LC_{50}" column indicates if there was enough data and the shape of the curve permitted us to calculate LC_{50} (see methods for more details). Models considered included linear (lm) and generalized additive (gam) models with abundance (ab), log(abundance + 1) (logab), log(Cl^- concentration + 1) (logcl), and both variables log-transformed (loglog). Table shows models within 2 ΔAIC and GAM models with log(abundance + 1).

Lake	Model	Delta AICc	Adjusted R^2	Used for LC_{50}
Paint	lm.loglog	0.00	0.482	N
Paint	**gam.logab**	**4.66**	**0.429**	**Y**
Long	lm.logab	0.00	0.228	N
Long	**gam.logab**	**0.00**	**0.228**	**Y**
Dartmouth	lm.logab	0.00	-0.044	N
Dartmouth	**gam.logab**	**0.00**	**-0.044**	**N**
Dartmouth	lm.loglog	0.18	-0.053	N
Purdue	lm.logab	0.00	0.048	N
Purdue	**gam.logab**	**0.00**	**0.048**	**Y**
Purdue	lm.loglog	1.11	0.012	N
Stortjärn	**gam.logab**	**0.00**	**0.761**	**Y**
Stortjärn	lm.logab	0.76	0.681	N
Croche	lm.loglog	0.00	0.289	N
Croche	**gam.logab**	**8.49**	**0.464**	**N**
George	**gam.logab**	**0.00**	**0.396**	**Y**
Opeongo	**gam.logab**	**0.00**	**0.833**	**Y**
Kraus	lm.loglog	0.00	0.020	N
Kraus	lm.logab	0.18	0.014	N
Kraus	**gam.logab**	**0.18**	**0.014**	**N**
Hertel	lm.logab	0.00	0.543	N

Hertel	**gam.logab**	**0.00**	**0.543**	**Y**
KBS Reservoir	lm.logab	0.00	-0.004	N
KBS Reservoir	**gam.logab**	**0.00**	**-0.004**	**N**
KBS Reservoir	lm.loglog	0.99	-0.052	N
Feresjön	lm.loglog	0.00	0.172	N
Feresjön	lm.logab	1.65	0.096	N
Feresjön	**gam.logab**	**2.67**	**0.120**	**Y**
Erken	**gam.logab**	**0.00**	**0.575**	**N**
Convict	lm.logab	0.00	-0.024	N
Convict	**gam.logab**	**0.00**	**-0.024**	**N**
Convict	lm.loglog	0.33	-0.035	N
Tavernoles	**gam.logab**	**0.00**	**0.850**	**Y**

Table 4.5. Model selection table for chlorophyll a concentration, including adjusted R^2 and delta AICc values and whether the relationship was used to predict an LC_{50}. Models considered included linear and generalized additive (GAM) models with chlorophyll abundance (chl), log(abundance + 1) (logchl), log(Cl^- concentration + 1) (logcl), and both variables log-transformed. Table shows models within 2 ΔAIC and GAM models with log(abundance + 1).

Lake	Model	Delta AICc	Adjusted R^2
Paint	**gam.chl**	**0.00**	**0.379**
Long	lm.logchl	0.00	0.192
Long	**gam.chl**	**2.77**	**0.233**
Dartmouth	lm.chl	0.00	0.089
Dartmouth	**gam.chl**	**0.00**	**0.089**
Dartmouth	lm.logchl	0.89	0.094
Sturgeon	lm.chl	0.00	0.020
Sturgeon	**gam.chl**	**0.00**	**0.020**
Sturgeon	lm.logchl	0.73	-0.029
Purdue	**gam.chl**	**0.00**	**0.772**
Purdue	lm.chl	1.21	0.294
Stortjärn	lm.logchl	0.00	0.156
Stortjärn	lm.chl	1.80	0.051
Stortjärn	**gam.chl**	**2.68**	**0.401**
Croche	lm.logchl	0.00	-0.050
Croche	lm.chl	0.08	-0.048
Croche	**gam.chl**	**0.08**	**-0.048**
George	lm.chl	0.00	0.111
George	**gam.chl**	**0.00**	**0.111**
Opeongo	**gam.chl**	**0.00**	**0.320**
Kraus	lm.chl	0.00	0.164
Kraus	**gam.chl**	**0.00**	**0.164**
Hertel	lm.chl	0.00	-0.025

Hertel	lm.logchl	0.41	-0.057
Hertel	**gam.chl**	**0.53**	**0.386**
KBS Reservoir	lm.chl	0.00	0.002
KBS Reservoir	**gam.chl**	**0.00**	**0.002**
KBS Reservoir	lm.logchl	1.41	-0.011
Feresjön	lm.chl	0.00	0.347
Feresjön	**gam.chl**	**2.68**	**0.624**
Erken	lm.logchl	0.00	-0.019
Erken	lm.chl	0.26	-0.037
Erken	**gam.chl**	**1.88**	**0.063**
Convict	**gam.chl**	**0.00**	**0.920**
Tavernoles	lm.chl	0.00	0.129
Tavernoles	**gam.chl**	**0.35**	**0.294**

Table 4.6. Comparison of the global model of taxon abundance as a function of Cl^- compared to a model with lake-specific smooth relationships. Bolded models are the best fit model for each taxonomic group.

Taxa	Model	AIC	R^2_{adj}	Est. df	F	p
Cladoceran	s(chloride)	1241	0.66	5.1	68.2	<0.001
	s(chloride, by=lake)	**1124**	**0.77**			
Calanoid	s(chloride)	636	0.40	3.4	22.7	<0.001
	s(chloride, by=lake)	**618**	**0.47**			
Cyclopoid	s(chloride)	1086	0.68	1.9	70.6	<0.001
	s(chloride, by=lake)	**830**	**0.85**			
Rotifer	s(chloride)	1324	0.58	4.7	10.2	<0.001
	s(chloride, by=lake)	1172	**0.75**			

Table 4.7. GAM results for the models with site-specific smooth relationships between taxon abundance and Cl^- including the estimated degrees of freedom (edf), F-values, and p-values for each smoothed term. Bolded relationships are significant at p<0.05.

	Cladocerans			Calanoids			Cyclopoids			Rotifer		
	edf	F	p	edf	F	p	edf	F	p	edf	F	p
Paint	**2.6**	**22.7**	**<0.001**	1	0.5	0.4846	**5.1**	**12.8**	**<0.001**	**5.9**	**7.3**	**<0.001**
Long	**2**	**11.8**	**<0.001**				1	0	0.854	**1**	**12.6**	**<0.001**
Dartmouth	**1**	**34.4**	**<0.001**	1.3	2.4	0.057	1.1	1.4	0.1971	1.3	0.2	0.725
Sturgeon	**3.7**	**34.8**	**<0.001**	**3**	**6**	**<0.001**	**3.9**	**70.2**	**<0.001**			
Purdue	**1.1**	**64.8**	**<0.001**				1.9	1.5	0.255	1	2.3	0.1281
Stortjärn	**3.2**	**28.4**	**<0.001**	**1**	**9.5**	**0.0022**	1.3	1.4	0.1779	**1.8**	**14.4**	**<0.001**
Croche	**2.1**	**6.5**	**0.001**	**2.1**	**4.3**	**0.0158**	1	0.6	0.4526	3.9	0.9	0.3215
George	**6.6**	**8.5**	**<0.001**	1	0.8	0.3787	**1**	**6.5**	**0.011**	**6.7**	**6.7**	**<0.001**
Opeongo	**5**	**7.7**	**<0.001**	**2.3**	**11.6**	**<0.001**	**6.1**	**25.1**	**<0.001**	**5.6**	**17.9**	**<0.001**
Kraus	**1**	**30**	**<0.001**	**4.9**	**3.5**	**0.002**	**1**	**17.8**	**<0.001**	1	2.3	0.1289
Hertel	**1**	**17.6**	**<0.001**				1	0.3	0.5935	**1**	**8.8**	**0.0033**
KBS Reservoir	**3.3**	**18.4**	**<0.001**	**2.5**	**11**	**<0.001**	**2**	**20.7**	**<0.001**	1	0.5	0.4821
Feresjön	**2.9**	**8.4**	**<0.001**	1	0.7	0.4025	**4.5**	**12.9**	**<0.001**	1.1	1.7	0.151
Erken	**2.1**	**4.7**	**0.008**	**2.6**	**4.7**	**0.0022**	3.2	1.9	0.1031	**4.2**	**9**	**<0.001**
Convict	**3.2**	**14.6**	**<0.001**	1	0.3	0.5672	**2.7**	**6.9**	**<0.001**	1	0	0.9553
Tavernoles							**5.5**	**3.9**	**<0.001 6**	**2.1**	**4.5**	**0.0089**

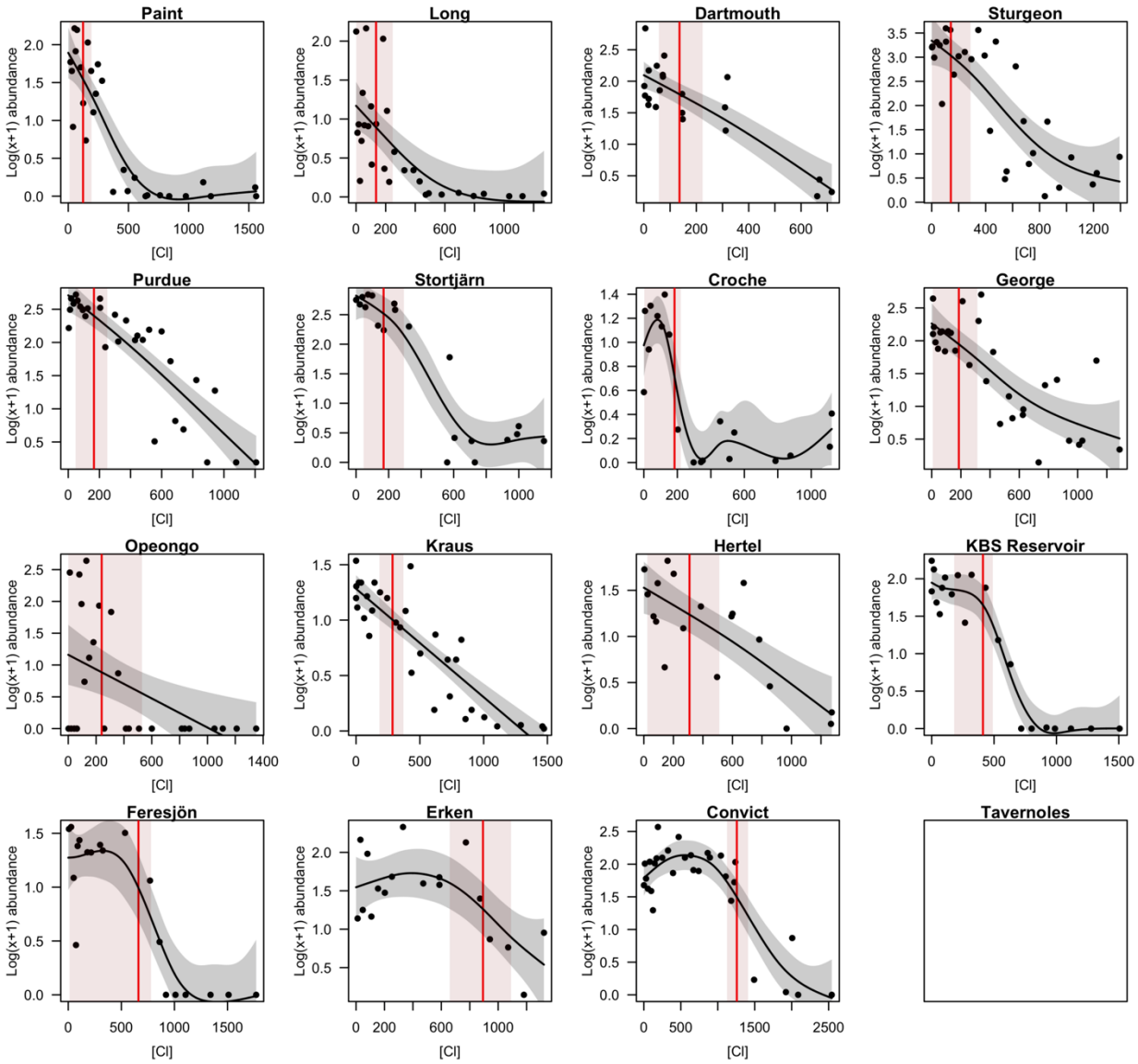

Figure 4.1. Predicted relationship between log10(x+1) cladoceran abundance and Cl^- concentration using generalized additive models (GAMs) for 15 study sites throughout North America and Europe. Red vertical line indicates the LC_{50} value for each site with the associated 95% confidence intervals (shaded region around the vertical line). Cladocerans were not detected in the experiment at Tavernoles.

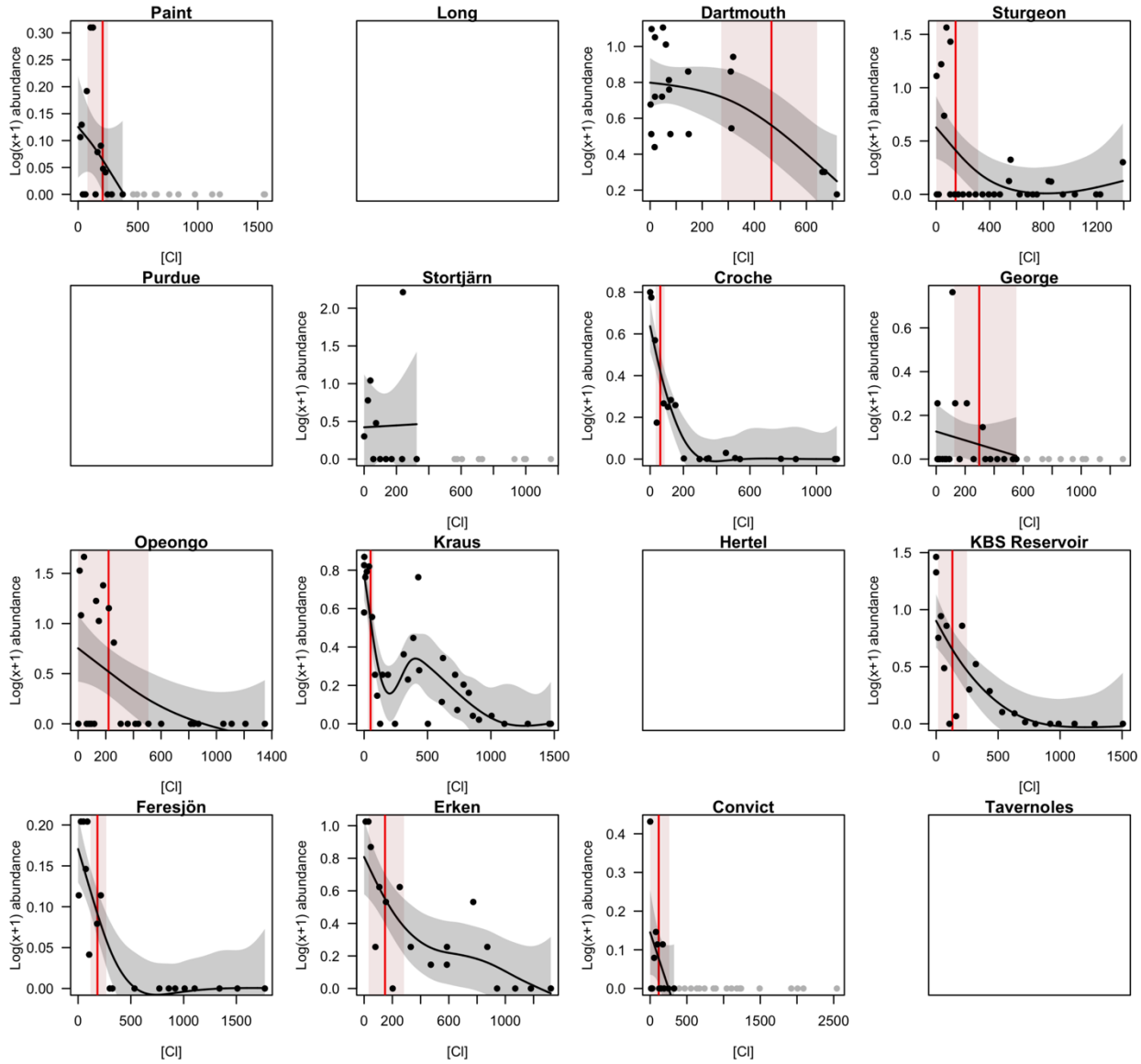

Figure 4.2. Predicted relationship between log10(x+1) calanoid abundance and Cl^- concentration using generalized additive models (GAMs) for 12 study sites throughout North America and Europe where calanoids were detected. Red vertical line indicates the LC_{50} value for each site with the associated 95% confidence intervals (shaded region around the vertical line). Points in gray were not used in fitting the GAMs; Cl^- gradients were truncated to improve model fit when the decline in abundance was steep and no individuals were detected at high Cl^- concentrations. LC_{50} was not estimated for Storjärn because the GAM model did not detect a change in abundance along the chloride gradient.

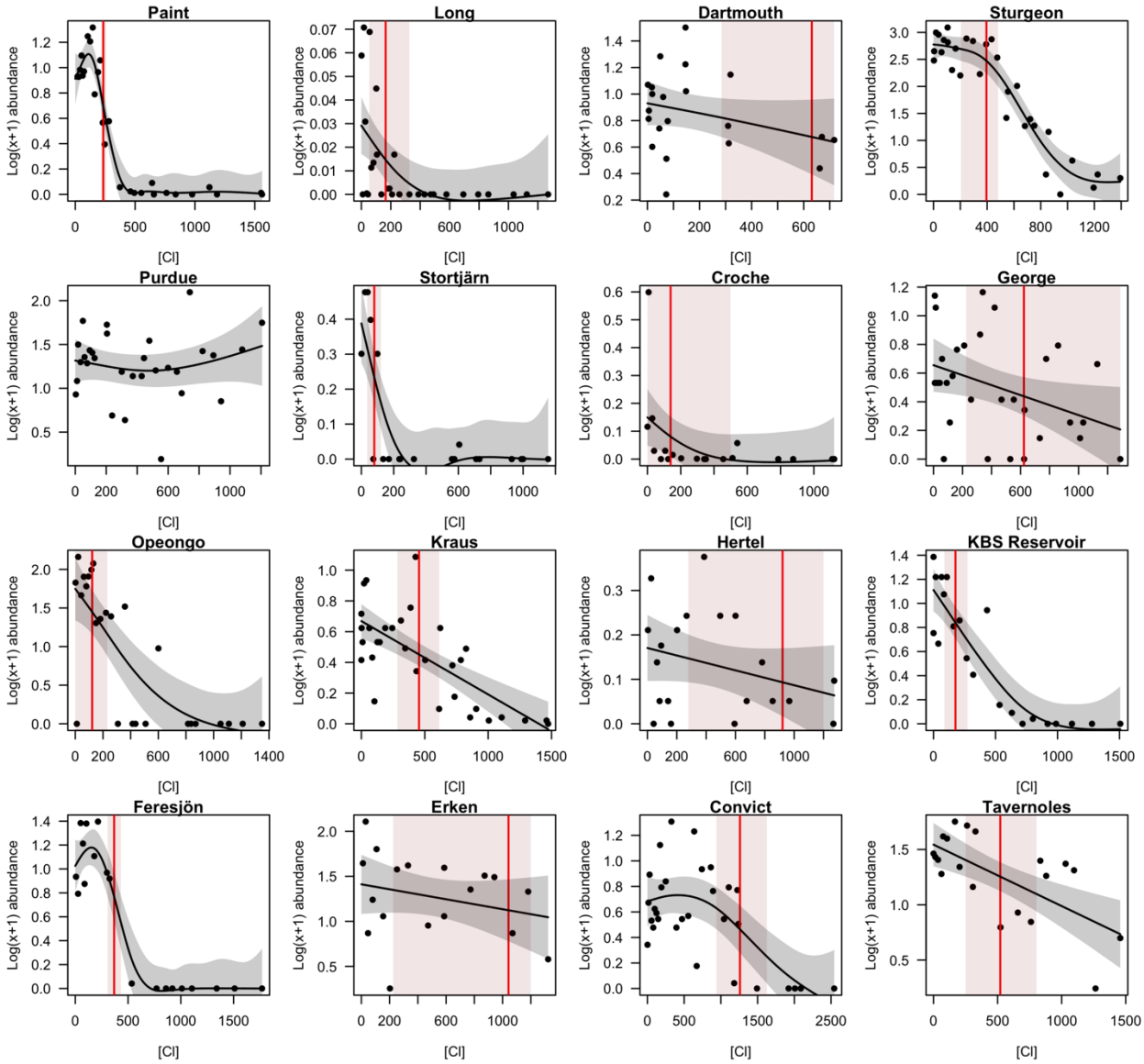

Figure 4.3. Predicted relationship between log10(x+1) cyclopoid abundance and Cl^- concentration using generalized additive models (GAMs) for 16 study sites throughout North America and Europe. Red vertical line indicates the LC_{50} value for each site with the associated 95% confidence intervals (shaded region around the vertical line). LC_{50} was not calculated for Purdue because abundance did not decline with increasing Cl^- concentration.

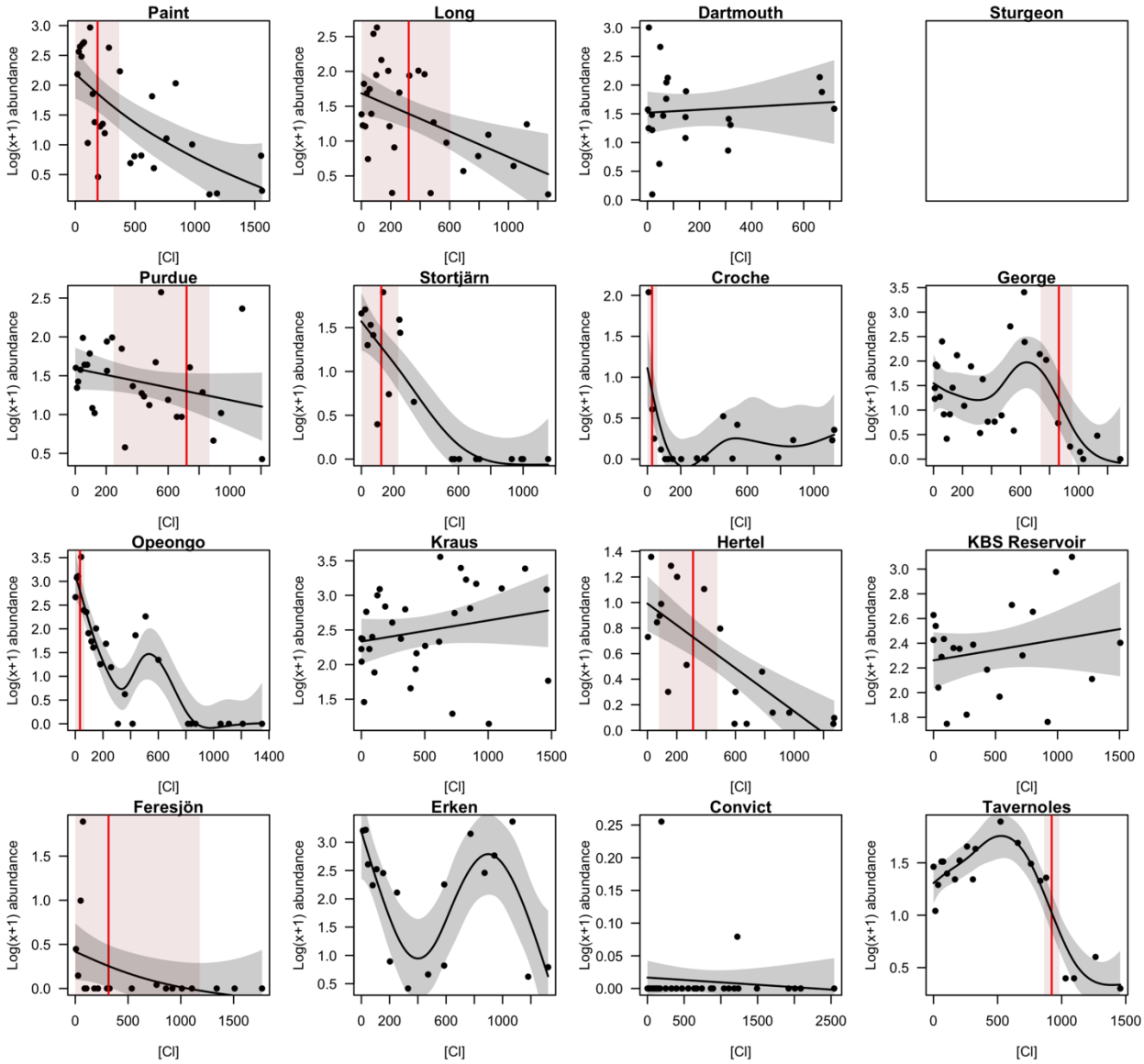

Figure 4.4. Predicted relationship between log10(x+1) rotifer abundance and Cl^- concentration using generalized additive models (GAMs) for 15 study sites throughout North America and Europe where rotifers were enumerated. Red vertical line indicates the LC_{50} value for each site with the associated 95% confidence intervals (shaded region around the vertical line). LC_{50} was not calculated for 5 sites because (1) there was no change in abundance with Cl^-, (2) there was an increase in abundance with Cl^- or (3) zooplankton abundance did not remain below 50% along the Cl^- gradient.

APPENDIX 5

Taxonomic keys and protocols for zooplankton identification:

Brooks, J. 1959. Cladocera. Pages 587–656 in H. Ward and G. Whipple, editors. Freshwater biology. John Wiley and Sons, New York, New York, USA.

DeMelo, R., and P. D. N. Hebert. 1994. A taxonomic reevaluation of North American Bosminidae. . *Canadian Journal of Zoology-Revue Canadienne De Zoologie*:1808–1825.

Dussart, B.H., Defaye, D., 1995. Introduction to the Copepoda. In: Guides to the Identification of the Microinvertebrates of the Continental Waters of the World (Dumont, H.J.F., Ed.), 7. SPB Academic Publishing, The Hague. 277 pp.

Dussart, B.H., Defaye, D., 2001. Introduction to the Copepoda. In: Guides to the Identification of the Microinvertebrates of the Continental Waters of the World (Dumont, H.J.F., Ed.). 2nd ed., Backhuys, Leiden. 344 pp.

Edmondson, W. 1960. Rotifera in Freshwater Biology. John Wiley and Sons, New York, New York, USA.

Haney, J.F. et al. "An-Image-based Key to the Zooplankton of North America" version 5.0 released 2013. University of New Hampshire Center for Freshwater Biology

Hebert, P. D. N. 1995. The Daphnia of North America: an illustrated fauna. CD-ROM. *University of Guelph, Guelph, Ontario, Canada*.

Hudson, P., and L. Lesko. 2003. Free-living and Parasitic Copepods of the Laurentian Great Lakes: keys and details on individual species. http://www.glsc.usgs.gov/greatlakescopepods/

Koste, W., 1978. Rotatoria. Die Rädertiere Mitteleuropas. Bd 1-2. Gebrüder Borntraeger, Berlin, Stuttgart.

Nogrady, T., 1982. Rotifera. In: Synopsis and Classification of Living Organisms (Parker, S.P., Ed.), pp. 865-872. McGraw-Hill Book Co., New York, NY.

Nogrady, T., Wallas, R.L., Snell, T.W., 1993. Biology, Ecology and Systematics. In: Rotifera (Nogrady, T., Ed.), Vol. 1, 142 pp. SPB Academic Publishing.

Smith, K., and F. C. H. 1978. A guide to the freshwater calanoid and cyclopoid copepod Crustacea of Ontario. Ser. No. 18, University of Waterloo, Department of Biology, Waterloo, Ontario, Canada.

Stemberger, R. 1979. A guide to rotifers of the Lauren- tian Great Lakes. Environmental Monitoring and Support Laboratory, Office of Research and Development, US Environmental Protection Agency, Washington, D.C., USA.

Stemberger, R. S., and J. J. Gilbert. 1987. Rotifer threshold food concentrations and the size-efficiency hypothesis. *Ecology* **68**:181-187.

Telesh, I.V., Heerkloss, R., 2002. Atlas of Estuarine Zooplankton of the Southern and Eastern Baltic Sea. Part I: Rotifera. Verlag Dr. Kovač, Hamburg. 89 pp.

Table 5.1. Mesocosm characteristics for site-specific set up and methods.

Lake	Mesocosm volume (L)	Number of mesocosms	Mesocosm type	Mesocosm cover	Nutrients added*
Paint	800	30	Land-based	Window screen	5% per day ambient N, P
Long	1570	30	In-lake	Window screen	5% per day ambient N, P
Dartmouth	121	21	Land-based	Window screen	Leaf bag added week 0
Sturgeon	200	30	Land-based	Window screen	No
Purdue	150	30	Land-based	Window screen	5% per day ambient N, P
Stortjärn	550	20	In-lake	None	No
Croche	2500	20	In-lake	Coarse mesh	5% per day ambient N, P
George	1000	30	Land-based	Shade cloth (60%)	5% per day ambient N, P
Opeongo	180	30	Land-based	Window screen	5% per day ambient N, P
Kraus	300	32	Land-based	Window screen	5% per day ambient N, P
Hertel	80	20	Land-based	Window screen	5% per day ambient N, P
KBS	345	21	Land-based	Window screen	5% per day ambient N, P
Feresjön	550	20	In-lake	None	No
Erken	550	20	In-lake	None	5% per day ambient N, P
Convict	1000	30	Land-based	Shade cloth (40%)	5% per day ambient N, P
Tavernoles	200	20	Land-based	Plastic cover	5% per day ambient N, P

*generally added every two weeks; weekly in George

Table 5.2. Zooplankton sampling and counting methods for the final day.

Lake	Sampling method	Mesh size (µm)	Volume sampled (L)	Counting protocol
Paint	12L *3 Schindler	50	36	250 ind.with <50 ind/sp. or until 3 subsamples yielded no new sp.
Long	15cm dia. net	50	177	250 ind.with <50 ind/sp. or until 3 subsamples yielded no new sp.
Dartmouth	Integrated tube	53	4	Entire sample
Sturgeon	15cm dia. net	50	8.8	Subsamples of 100 ind. repeated until CV<0.3
Purdue	Grab sample*3	50	14.4	12.5-100% of sample
Stortjärn	2.5L*6 Ruttner	55	10	10-100% of sample
Croche	35cm dia. net	54	106	>200 ind./sp OR 1000 total ind. OR entire sample
George	0.5L*24 grab	50	12	25% of sample with scan for rare species
Opeongo	2L*5 tube	50	10	>100 ind. or 5 subsamples
Kraus	Integrated tube	50	12	25-200% crustacean sample, 5% rotifer sample
Hertel	Integrated tube	53	8	Entire sample
KBS	10L grab	60	30	Subsamples until 75 ind./sp. counted
Feresjon	2.5L*6 Ruttner	50	10	Entire sample
Erken	2.5L*6 Ruttner	55	10	>250 ind.
Convict	Integrated tube	64	20	200 ind. with <50 per sp.
Tavernoles	Multiple 5L grab	50	30	Subsamples until most abundant taxa = 100 ind.

Table 5.3. Analytical methods. Fluor.=fluorometry, Spectro.=spectrophotometry

Lake	Conductivity probe	Chloride	Chlorophyll *a*
Paint	YSI 600XL	Dionex ICS1600 Ion chromatography	Fluor./methanol
Long	YSI 600R	Dionex ICS1600 Ion chromatography	Fluor./methanol
Dartmouth	YSI Pro DSS	Ion chromatography EPA method 300	Fluor./methanol
Sturgeon	YSI	Regression	Fluor./methanol
Purdue	Oakton PCSTestr	Ion chromatography EPA method 300	Fluor./ethanol
Stortjärn	Metrohm IC detector	IC Metrohm Net. V. 2.3 Ion Chromatography	LS 55 Fluor. Spectro.
Croche	YSI pro plus	Dionex DX-600 Ion chromatography	Spectro./ethanol
George	YSI pro plus	YSI pro plus	Fluor./acetone
Opeongo	YSI	Dionex ICS1600 Ion chromatography	Fluor./methanol
Kraus	YSI 6000	regression	Fluor./methanol
Hertel	YSI pro plus	Dionex DX-600 Ion chromatography	In vivo fluor.
KBS	Hydrolab HL4	regression	Fluor./ethanol
Feresjön	Hach HQ40D with CDC40103 probe	Metrohm IC system	LS 55 Fluor. Spectro.
Erken	YSI Exosonde	Metrohm IC system	Spectro./ethanol
Convict	YSI pro plus	Dionex ICS-2000 Ion chromatography	Fluor./acetone
Tavernoles	YSI pro plus	Standard Methods 4500 Cl B*	Spectro.

*BOE num.163 Ordre de 1 de juliol de 1987. 15871

APPENDIX 6

Tables and Figures for the principal components analysis (PCA) for water chemistry and zooplankton composition in control mesocosms.

Table 6.1. Analysis of variance results for cladoceran LC_{50} as a function of chemistry PC1 and PC2. Model = lm(LC_{50}_Cladoceran~ chem_PC1+ chem_PC2).

	Df	F value	Pr(>F)
chem_PC1	1	0.327	0.578
chem_PC2	1	0.318	0.583
Residuals	12		

Table 6.2. Analysis of variance results for cyclopoid copepod LC_{50} as a function of chemistry PC1 and PC2. Model = lm(LC_{50}_cyclopoid~ chem_PC1+ chem_PC2).

	Df	F value	Pr(>F)
chem_PC1	1	0.039	0.846
chem_PC2	1	0.993	0.339
Residuals	12		

Table 6.3. Analysis of variance results for calanoid LC_{50} as a function of chemistry PC1 and PC2. Model = lm(LC_{50}_calanoid~ chem_PC1+ chem_PC2).

	Df	F value	Pr(>F)
chem_PC1	1	0.351	0.570
chem_PC2	1	2.757	0.135
Residuals	8		

Table 6.4. Analysis of variance results for rotifer LC_{50} as a function of chemistry PC1 and PC2. Model = lm(LC_{50}_rotifer~ chem_PC1+ chem_PC2).

	Df	F value	Pr(>F)
chem_PC1	1	14.169	**0.007**
chem_PC2	1	9.740	**0.017**
Residuals	7		

Table 6.5. Analysis of variance results for cladoceran LC_{50} as a function of cladoceran PC1 and PC2. Model = lm(LC_{50}_Cladoceran~ clad_PC1+ clad_PC2).

	Df	F value	Pr(>F)
clad_PC1	1	0.146	0.710
clad_PC2	1	0.273	0.612
Residuals	12		

Table 6.6. Analysis of variance results for cyclopoid copepod LC_{50} as a function of cyclopoid PC1 and PC2. Model = lm(LC_{50}_cyclopoid~ cyc_PC1+ cyc_PC2).

	Df	F value	Pr(>F)
cyc_PC1	1	1.076	0.320
cyc_PC2	1	0.000	0.994
Residuals	11		

Table 6.7. Analysis of variance results for calanoid copepod LC_{50} as a function of calanoid PC1 and PC2. Model=lm(LC_{50}_calanoid~ cal_PC1+cal_PC2). The lowest AIC was associated with the model that only included the intercept.

	Df	F value	Pr(>F)
cal_PC1	1	0.182	0.681
cal_PC2	1	0.777	0.404
Residuals	8		

Table 6.8. Analysis of variance results for rotifer LC_{50} as a function of rotifer PC1 and PC2. Model=lm(LC_{50}_rotifer~ rot_PC1+rot_PC2).

	Df	F value	Pr(>F)
rot_PC1	1	0.036	0.855
rot_PC2	1	0.325	0.587
Residuals	7		

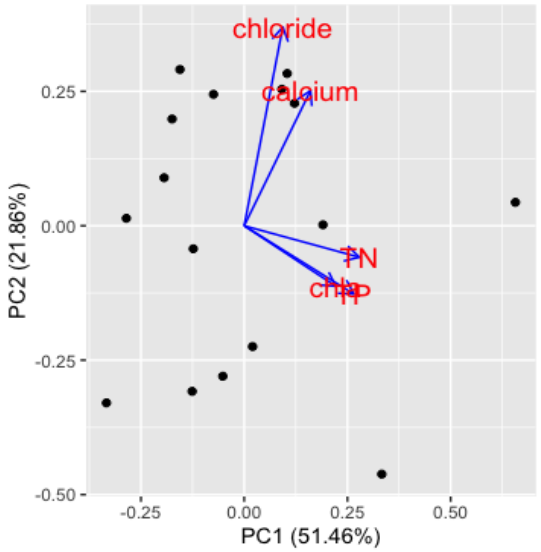

Figure 6.1. The first and second principal components for log_{10}-transformed water chemistry variables (Cl^-, Ca^{2+}, TN, TP, chl a), representing source lake conditions at each of the 16 sites.

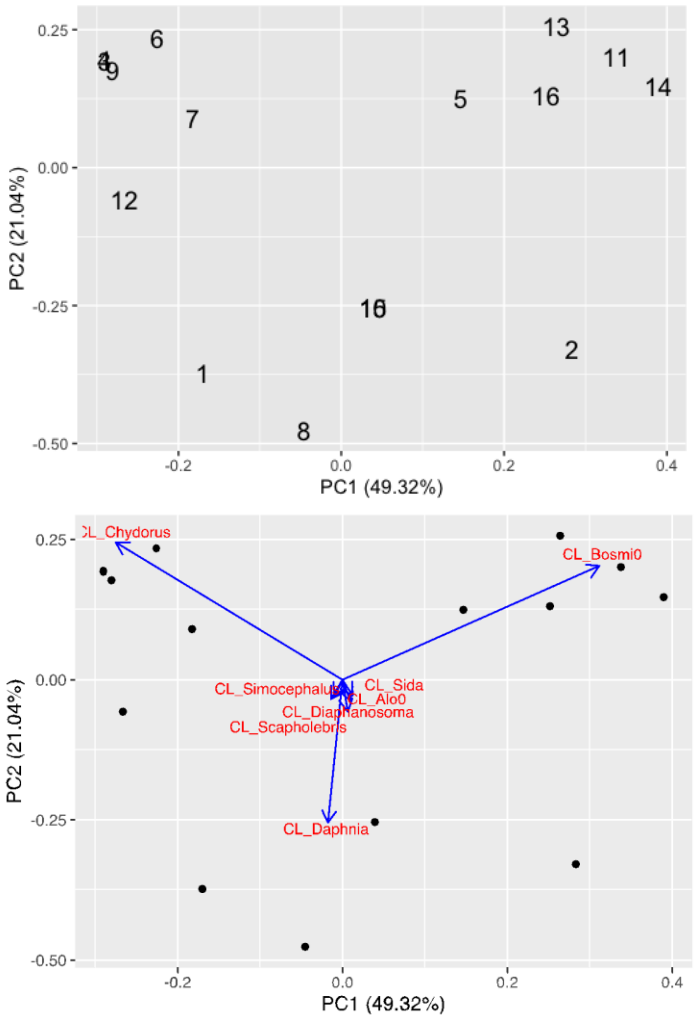

Figure 6.2. The first and second principal components for Hellinger-transformed cladocerans abundance in control meosocsms at each of the 16 sites. 1=Convict, 2=Croche, 3=Dartmouth, 4=Erken, 5=Feresjön, 6=George, 7 Hertel, 8=KBS, 9=Kraus, 10=Long, 11 = Opeongo, 12=Paint, 13=Purdue, 14=Stortjärn, 15= Sturgeon, 16=Tavernoles.

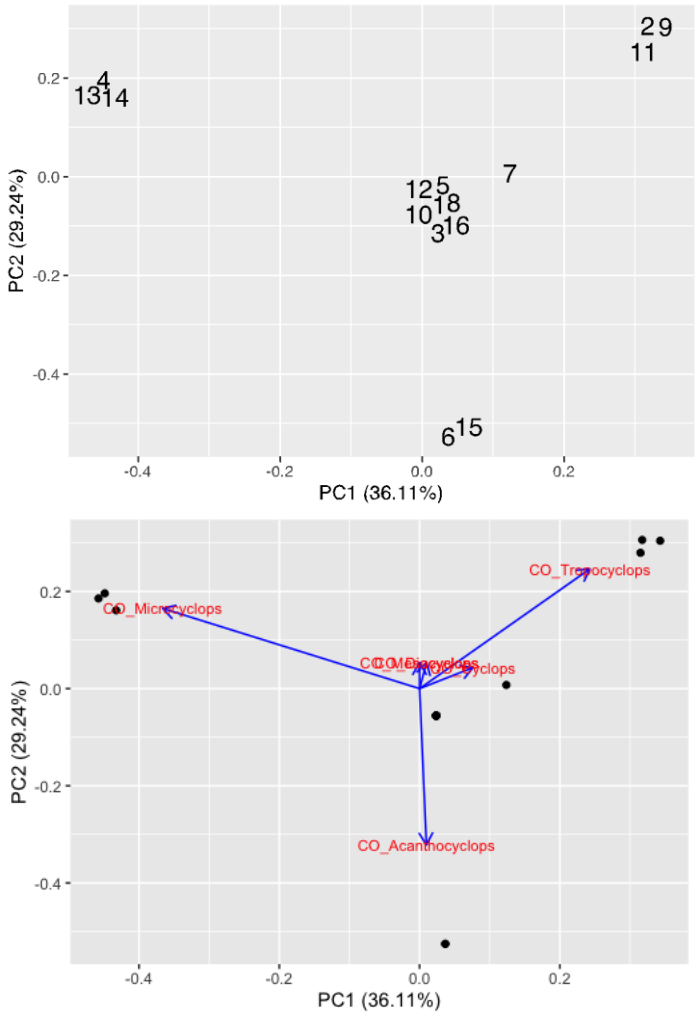

Figure 6.3. The first and second principal components for Hellinger-transformed cyclopoid copepod abundance in control meosocsms at each of the 16 sites. 1=Convict, 2=Croche, 3=Dartmouth, 4=Erken, 5=Feresjön, 6=George, 7 Hertel, 8=KBS, 9=Kraus, 10=Long, 11 = Opeongo, 12=Paint, 13=Purdue, 14=Stortjärn, 15= Sturgeon, 16=Tavernoles. Lake numbers have been jiddered for display.

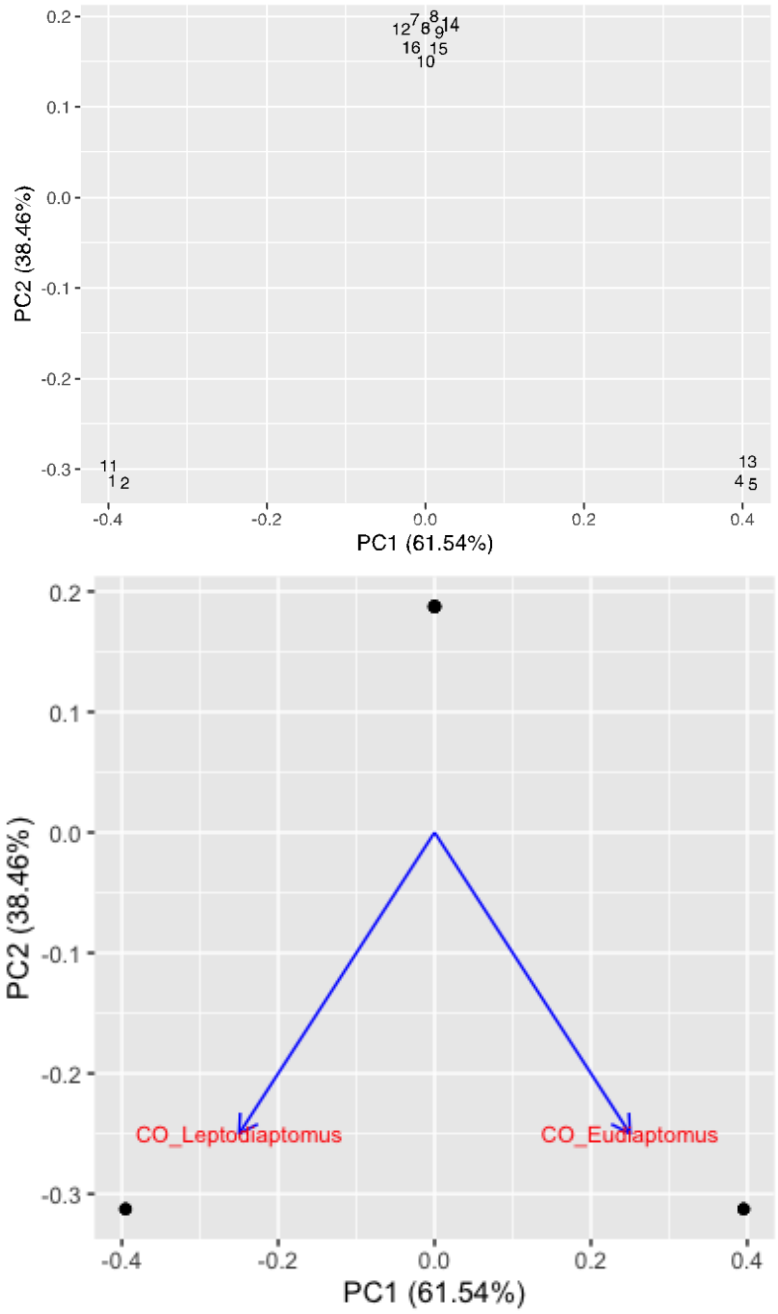

Figure 6.4. The first and second principal components for Hellinger-transformed calanoids abundance in control meosocsms at each of the 16 sites. 1=Convict, 2=Croche, 3=Dartmouth, 4=Erken, 5=Feresjön, 6=George, 7 Hertel, 8=KBS, 9=Kraus, 10=Long, 11 = Opeongo, 12=Paint, 13=Purdue, 14=Stortjärn, 15= Sturgeon, 16=Tavernoles. Lake numbers have been jittered for display.

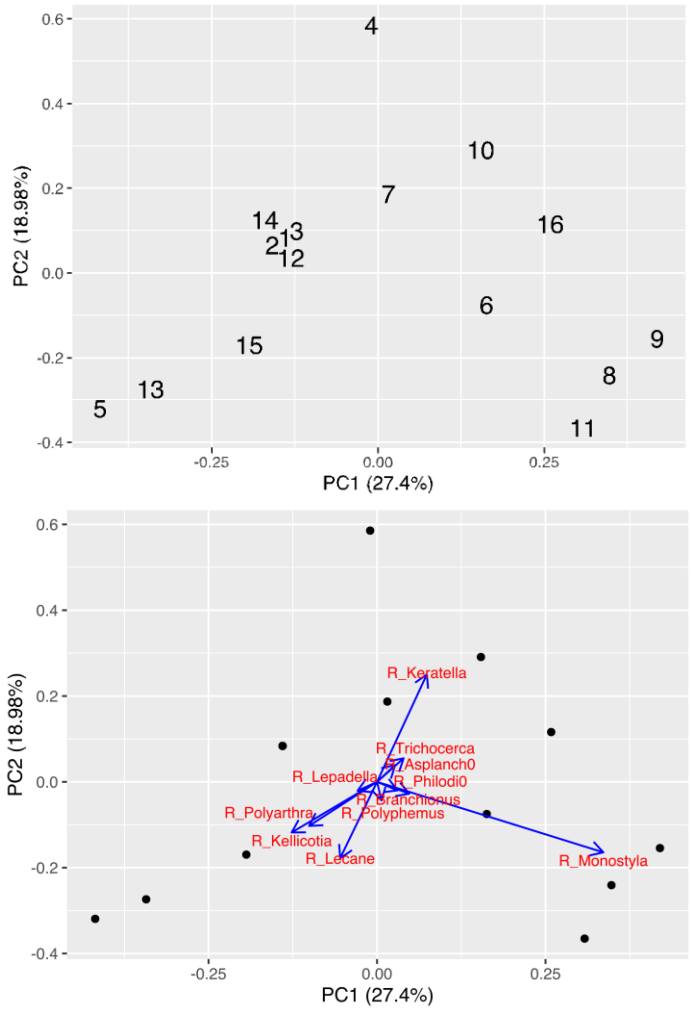

Figure 6.5. The first and second principal components for Hellinger-transformed rotifers abundance in control meosocsms at each of the 16 sites. 1=Convict, 2=Croche, 3=Dartmouth, 4=Erken, 5=Feresjön, 6=George, 7 Hertel, 8=KBS, 9=Kraus, 10=Long, 11 = Opeongo, 12=Paint, 13=Purdue, 14=Stortjärn, 15= Sturgeon, 16=Tavernoles.